Acta Crystallographica Section C
Crystal Structure Communications
ISSN 0108-2701

6-[(4-Fluorophenyl)(1*H*-imidazol-1-yl)-methyl]-1,3-benzodioxol-5-ol and 6-[(4-methoxyphenyl)(1*H*-imidazol-1-yl)methyl]-1,3-benzodioxol-5-ol

L. C. R. Andrade,[a] J. A. Paixão,[a]* M. J. M. de Almeida,[a] M. A. C. Neves[b] and M. L. Sá e Melo[b]

[a]CEMDRX, Departamento de Física, Faculdade de Ciências e Tecnologia, Universidade de Coimbra, P-3004-516 Coimbra, Portugal, and [b]Centro de Estudos Farmacêuticos, Laboratório de Química Farmacêutica, Faculdade de Farmácia, Universidade de Coimbra, P-3000-548 Coimbra, Portugal
Correspondence e-mail: jap@pollux.fis.uc.pt

Received 14 July 2010
Accepted 28 August 2010
Online 10 September 2010

The title compounds, $C_{17}H_{13}FN_2O_3$ and $C_{18}H_{16}N_2O_4$, are new potent aromatase inhibitors combining the common features of second- and third-generation nonsteroid anti-aromatase compounds. The molecules have a propeller shape, with dihedral angles between adjacent planes in the range 49–86°. A quantum mechanical *ab initio* Roothaan–Hartree–Fock calculation for the isolated molecules shows values for these angles close to the ideal value of 90°. Docking studies of the molecules in the aromatase substrate show that their strong inhibitor potency can be attributed to molecular flexibility, hydrophobic interactions, heme Fe coordination and hydrogen bonding.

Comment

The title compounds, (I) and (II), respectively, are new potent aromatase inhibitors identified *in silico* using a fast high-throughput screening methodology based on a pharmacophore model combining the common features of second- and third-generation nonsteroid anti-aromatase compounds (Neves *et al.*, 2009). Their inhibition activity was confirmed *in vitro* using a biochemical assay with aromatase extracted from human term placenta (Neves *et al.*, 2007). Both compounds were able to block the enzyme with strong potency [for compound (I), IC_{50} = 5.3 n*M*, and for compound (II), IC_{50} = 55 n*M*] and a competitive mechanism of inhibition. Letrozole, a third-generation aromatase inhibitor, was tested under the same assay conditions, showing IC_{50} = 6.1 n*M*. The unique structure and strong aromatase potency of these new compounds makes them interesting candidates for lead optimization, hence the importance of their accurate structure determination from both X-ray diffraction and molecular quantum mechanical calculations. As compounds (I) and (II) compete with testosterone and androstenedione for the active site of aromatase, docking studies using the X-ray crystal structure of the enzyme (Ghosh *et al.*, 2009) will further contribute to the understanding of the evidenced strong inhibitory potency.

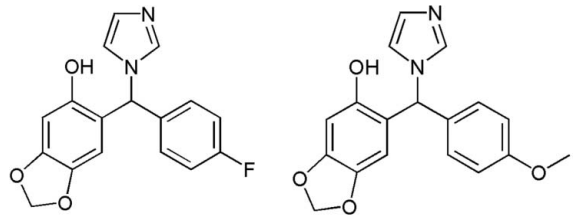

(I) (II)

X-ray diffraction studies of (I) and (II) led to the molecular structures depicted in Figs. 1 and 2, respectively. Average bond lengths are within normal ranges (Allen *et al.*, 1987) for both molecules, except for those of the substituted phenyl rings, where the averages of the C—C bonds are shorter than the usual value of 1.395 Å [1.369 Å for (I) and 1.372 Å for (II)]. In addition, the C—C distances differ significantly within these

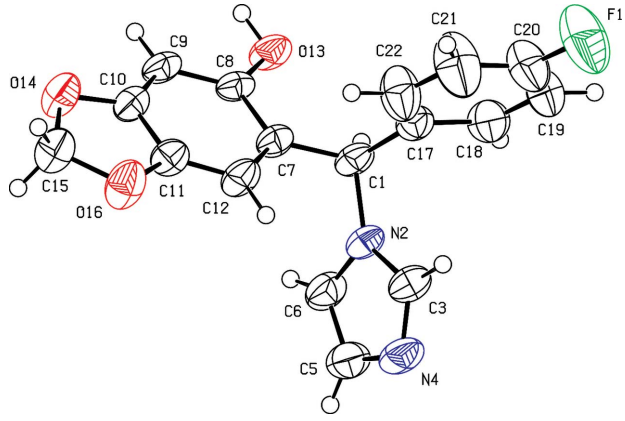

Figure 1
The structure of (I), showing the atom-numbering scheme. Displacement ellipsoids are drawn at the 50% probability level and H atoms are shown as small spheres of arbitrary radii.

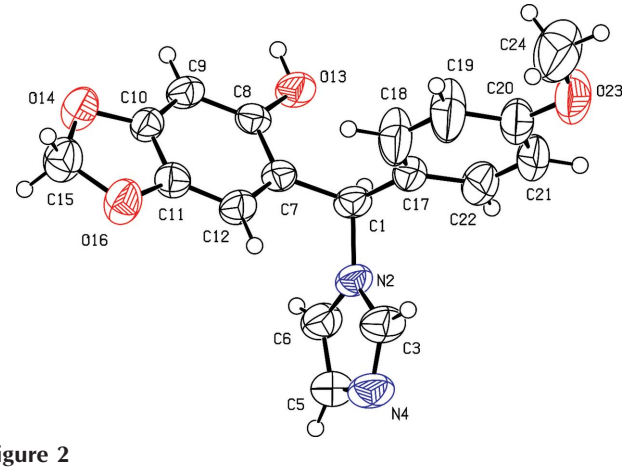

Figure 2
The structure of (II), showing the atom-numbering scheme. Displacement ellipsoids are drawn at the 50% probability level and H atoms are shown as small spheres of arbitrary radii.

 doi:10.1107/S0108270110034773

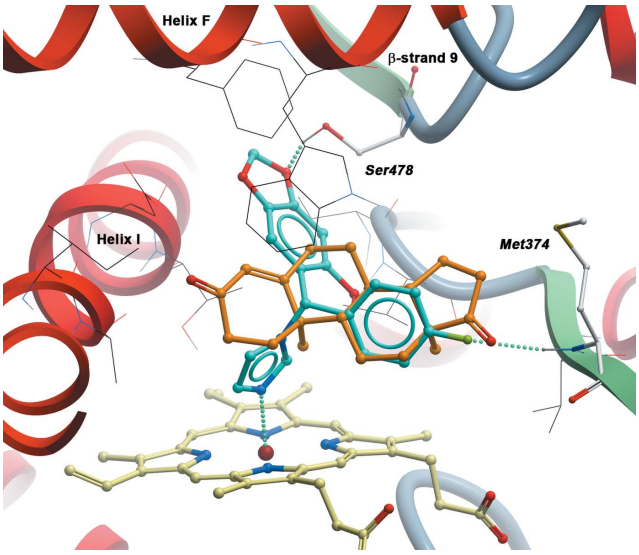

Figure 3
The docking of (I) within the aromatase active site.

rings. In fact, the C19—C20 and C20—C21 bond lengths are significantly shorter than the remaining fluorophenyl and methoxyphenyl ones (see Tables 1 and 4). Also, for the benzodioxole part, C9—C10 and C11—C12 are significantly shorter than neighbouring bonds not involved in the attached five-membered ring. One possible explanation could be the effect of thermal motion of the atoms involved in these bonds, which tends to shorten the observed distances, but correcting these distances by applying a rigid-body motion analysis using a **TLS** model (Schomaker & Trueblood, 1968) [1.372 Å for (I) and 1.375 Å for (II)] is not sufficient to recover the nominal average value for aromatic C—C bonds. Both molecules have propeller structures, as evidenced by the dihedral angles given in Tables 3 and 6.

The cohesion of the structures of (I) and (II) involves strong hydrogen bonds between the hydroxy groups, acting as donors, and atoms N4 of the imidazole rings, acting as acceptors. In both compounds, the hydrogen-bonding pattern is that of chains, running along the *c* axis in (I) and the *b* axis in (II) (Tables 2 and 5).

In order to gain some insight into how the crystal packing of the molecules might affect their molecular geometry, and to compare the geometry of the free molecules with those adapted to the docking site, we have also performed a quantum chemical calculation on the equilibrium geometry of the isolated molecules. We were also interested in checking whether the observed deviations in the C—C bonds of the aromatic rings could be reproduced. These calculations were performed with the computer program *GAMESS* (Schmidt *et al.*, 1993). A molecular orbital Roothan–Hartree–Fock method was used with an extended 6–31G(d,p) basis set. Tight conditions for convergence of both the self-consistent field cycles and maximum density and energy gradient variations were imposed (10^{-6} atomic units). The program was run on the Milipeia cluster at UC–LCA (16 Opteron cores, 2.2 GHz, running Linux).

Docking studies using the X-ray crystal structure of aromatase (Ghosh *et al.*, 2009) showed that, when bound to the active site, the studied molecules (I) and (II) adopt a conformation in which the hydrophobic diphenylmethane scaffold partially overlaps with the steroid hydrophobic framework and the N-containing heterocycle points in a similar direction in space to that of the steroid 19-methyl, coordinating with the heme Fe atom (Fig. 3). The hydrophobic scaffolds of compounds (I) and (II) are remarkably complemented by apolar residues within the aromatase active site, whereas either the fluorine or methoxy and the dioxole groups interact with hydrogen-bond donors. The backbone amide of methionine 374, involved in a hydrogen bond with the substrate 17-keto O atom in the crystal structure (Ghosh *et al.*, 2009), will likely interact with one of the acceptor groups, aligning the corresponding phenyl moiety with steroid ring *C*. A new pocket, defined at the helix F, helix I and β-strand 9 interfaces, is occupied by the second phenyl moiety, and a hydrogen bond is established with serine 478.

The results of the *ab initio* calculations for the free molecules show the high degree of rotational flexibility of the three ring planes of the propeller configuration, which is also important for good docking to the active site of aromatase (Tables 3 and 6). In the free state, the dihedral angles are close to 90°, as expected from the minimization of the steric interaction between adjacent rings. In both the observed crystal conformations and the adapted docking geometries, these angles are substantially smaller, due to packing and intramolecular interactions. Interestingly, the *ab initio* calculations reproduce the observed short C9—C10 and C11—C12 bond distances compared with the average aromatic values, although the same is not true for the C19—C20 and C20—C21 bonds.

In summary, rotational molecular flexibility, hydrophobic interactions, heme Fe coordination and hydrogen bonding are the main driving forces for strong aromatase binding, explaining the high potency of the studied compounds.

Experimental

Compounds (I) and (II) were obtained from the Drug Synthesis and Chemistry Branch, Developmental Therapeutics Program, Division of Cancer Treatment and Diagnosis of the US National Cancer Institute. The purity of the samples was evaluated by elemental analysis. Compound (I): C 65.38, H 4.20, N 8.97% (calculated); C 65.92, H 4.35, N 8.88% (found). Compound (II): C 66.66, H 4.97, N 8.64% (calculated); C 66.72, H 5.17, N 8.54% (found). The crystals used for analysis were taken directly from the provided samples.

Compound (I)

Crystal data

$C_{17}H_{13}FN_2O_3$
M_r = 312.29
Monoclinic, $P2_1/c$
a = 7.5621 (2) Å
b = 24.0471 (6) Å
c = 8.8524 (2) Å
β = 111.966 (1)°
V = 1492.92 (6) Å^3
Z = 4
Mo $K\alpha$ radiation
μ = 0.11 mm^{-1}
T = 293 K
0.42 × 0.22 × 0.20 mm

Table 1
Selected bond lengths (Å) for (I).

C7—C8	1.3939 (19)	C17—C22	1.369 (3)
C7—C12	1.398 (2)	C17—C18	1.391 (2)
C8—C9	1.401 (2)	C18—C19	1.375 (3)
C9—C10	1.354 (2)	C19—C20	1.345 (3)
C10—C11	1.374 (2)	C20—C21	1.351 (3)
C11—C12	1.360 (2)	C21—C22	1.381 (3)

Table 2
Hydrogen-bond geometry (Å, °) for (I).

D—H···*A*	*D*—H	H···*A*	*D*···*A*	*D*—H···*A*
O13—H13···N4^{i}	0.82	1.88	2.6947 (17)	175

Symmetry code: (i) $x, y, z-1$.

Table 3
Comparison of geometric parameters for selected distances (Å) and dihedral angles (°) for (I).

A is the imidazole ring, *B* the dioxole ring and *C* the fluorophenyl ring.

	X-ray data	*Ab initio* model	Docking model
C9—C10	1.354 (2)	1.367	1.377
C11–C12	1.360 (2)	1.364	1.381
C19—C20	1.345 (3)	1.380	1.389
C20—C21	1.351 (3)	1.375	1.389
A/*B*	80.91 (9)	85.37	68.64
B/*C*	74.95 (5)	88.87	75.50
A/*C*	48.87 (9)	89.43	66.24

Data collection

Bruker APEXII CCD area-detector diffractometer
Absorption correction: multi-scan (*SADABS*; Sheldrick, 2000)
T_{min} = 0.894, T_{max} = 0.979
32248 measured reflections
3406 independent reflections
2328 reflections with $I > 2\sigma(I)$
R_{int} = 0.026

Refinement

$R[F^2 > 2\sigma(F^2)]$ = 0.044
$wR(F^2)$ = 0.125
S = 1.04
3406 reflections
209 parameters
H-atom parameters constrained
$\Delta\rho_{max}$ = 0.17 e Å^{-3}
$\Delta\rho_{min}$ = −0.24 e Å^{-3}

Compound (II)

Crystal data

$C_{18}H_{16}N_2O_4$
M_r = 324.33
Triclinic, $P\overline{1}$
a = 7.6404 (2) Å
b = 8.8734 (2) Å
c = 13.0368 (3) Å
α = 100.627 (1)°
β = 91.113 (1)°
γ = 109.804 (1)°
V = 814.10 (3) Å^3
Z = 2
Mo $K\alpha$ radiation
μ = 0.10 mm^{-1}
T = 293 K
0.25 × 0.18 × 0.14 mm

Data collection

Bruker APEXII CCD area-detector diffractometer
Absorption correction: multi-scan (*SADABS*; Sheldrick, 2000)
T_{min} = 0.914, T_{max} = 0.987
15530 measured reflections
3738 independent reflections
2069 reflections with $I > 2\sigma(I)$
R_{int} = 0.024

Table 4
Selected bond lengths (Å) for (II).

C7—C8	1.385 (2)	C17—C18	1.363 (3)
C7—C12	1.399 (2)	C17—C22	1.381 (2)
C8—C9	1.397 (2)	C18—C19	1.387 (3)
C9—C10	1.362 (2)	C19—C20	1.364 (3)
C10—C11	1.372 (2)	C20—C21	1.362 (3)
C11—C12	1.361 (2)	C21—C22	1.374 (3)

Table 5
Hydrogen-bond geometry (Å, °) for (II).

D—H···*A*	*D*—H	H···*A*	*D*···*A*	*D*—H···*A*
O13—H13···N4^{i}	0.82	1.88	2.6949 (19)	175

Symmetry code: (i) $x, y+1, z$.

Table 6
Comparison of geometric parameters for selected distances (Å) and dihedral angles (°) for (II).

A is the imidazole ring, *B* the dioxole ring and *C* the methoxyphenyl ring.

	X-ray data	*Ab initio* model	Docking model
C9—C10	1.362 (2)	1.367	1.375
C11–C12	1.361 (2)	1.364	1.381
C19—C20	1.364 (3)	1.383	1.396
C20—C21	1.362 (3)	1.395	1.393
A/*B*	85.99 (9)	85.04	76.10
B/*C*	79.09 (10)	87.99	75.55
A/*C*	74.78 (12)	89.55	74.32

Refinement

$R[F^2 > 2\sigma(F^2)]$ = 0.046
$wR(F^2)$ = 0.130
S = 1.00
3738 reflections
219 parameters
H-atom parameters constrained
$\Delta\rho_{max}$ = 0.15 e Å^{-3}
$\Delta\rho_{min}$ = −0.19 e Å^{-3}

GOLD (Version 3.2; Verdonk *et al.*, 2003) was used to perform flexible docking of (I) and (II) into the binding pocket of the aromatase X-ray crystal structure (PDB entry 3eqm). The androstenedione substrate was removed and used to define the binding site as a 10 Å sphere above the heme group. An octahedral coordinating geometry was assigned to the heme Fe atom and the GOLDScore fitness function was used with metal parameters optimized for P450 enzymes, taking account of different hydrogen-bond acceptor types (Kirton *et al.*, 2005). Distance constraints were applied in order to keep the coordination between the imidazole N and the heme Fe atom within lower and upper limits of 1.9 and 2.5 Å, respectively. A total of 100 independent docking runs were performed with the default genetic algorithm search parameters.

Hydroxy H atoms were initially located in difference Fourier maps, then their positions were geometrically optimized and refined as riding on their parent O atoms while being allowed to rotate about the parent C—O bond [AFIX 147 instruction in *SHELXL97* (Sheldrick, 2008)], with U_{iso}(H) = 1.5U_{eq}(O). All other H atoms were placed in calculated idealized positions and refined as riding on their parent atoms, with C—H = 0.93–0.98 Å and U_{iso}(H) = 1.2U_{eq}(C), except for methyl groups for which U_{iso}(H) = 1.5U_{eq}(C).

For both compounds, data collection: *APEX2* (Bruker, 2006); cell refinement: *SAINT* (Bruker, 2003); data reduction: *SAINT*; program(s) used to solve structure: *SHELXS97* (Sheldrick, 2008);

program(s) used to refine structure: *SHELXL97* (Sheldrick, 2008); molecular graphics: *ORTEPII* (Johnson, 1976); software used to prepare material for publication: *SHELXL97*.

This work was supported by the Fundação para a Ciência e Tecnologia through a Financiamento Plurianual grant. We gratefully acknowledge the UC–LCA for granting computer time in the Milipeia cluster, and Mr Carlos Pereira for help in the analysis of the output of the *GAMESS* code.

Supplementary data for this paper are available from the IUCr electronic archives (Reference: SK3380). Services for accessing these data are described at the back of the journal.

References

Allen, F. H., Kennard, O., Watson, D. G., Brammer, L., Orpen, A. G. & Taylor, R. (1987). *J. Chem. Soc. Perkin Trans. 2*, pp. S1–19.

Bruker (2003). *SMART* and *SAINT*. Bruker AXS Inc., Madison, Wisconsin, USA.

Bruker (2006). *APEX2*. Bruker AXS Inc., Madison, Wisconsin, USA.

Ghosh, D., Griswold, J., Erman, M. & Pangborn, W. (2009). *Nature (London)*, **457**, 219–223.

Johnson, C. K. (1976). *ORTEPII*. Report ORNL-5138. Oak Ridge National Laboratory, Tennessee, USA.

Kirton, S. B., Murray, C. W., Verdonk, M. L. & Taylor, R. D. (2005). *Proteins*, **58**, 836–844.

Neves, M. A. C., Dinis, T. C. P., Colombo, G. & Melo, M. L. S. (2007). *ChemMedChem*, **2**, 1750–1762.

Neves, M. A. C., Dinis, T. C. P., Colombo, G. & Melo, M. L. S. (2009). *J. Med. Chem.* **52**, 143–150.

Schmidt, M. W., Baldrige, K. K., Boatz, J. A., Elbert, S. T., Gordon, M. S., Jensen, J. J., Koseki, S., Matsunaga, N., Nguyen, K. A., Sue, S., Windus, T. L., Dupuis, M. & Montgomery, J. A. (1993). *J. Comput. Chem.* **14**, 1347–1363.

Schomaker, V. & Trueblood, K. N. (1968). *Acta Cryst.* B**24**, 63–76.

Sheldrick, G. M. (2000). *SADABS*. University of Göttingen, Germany.

Sheldrick, G. M. (2008). *Acta Cryst.* A**64**, 112–122.

Verdonk, M. L., Cole, J. C., Hartshorn, M. J., Murray, C. W. & Taylor, R. D. (2003). *Proteins*, **52**, 609–623.